

A Multi-Stage Algorithm for Acoustic Physical Model Parameters Estimation

Leonardo Gabrielli, Stefano Tomassetti, Stefano Squartini, Carlo Zinato, Stefano Guaiana

Abstract—One of the challenges in computational acoustics is the identification of models that can simulate and predict the physical behavior of a system generating an acoustic signal. Whenever such models are used for commercial applications an additional constraint is the time-to-market, making automation of the sound design process desirable. In previous works, a computational sound design approach has been proposed for the parameter estimation problem involving timbre matching by deep learning, which was applied to the synthesis of pipe organ tones. In this work we refine previous results by introducing the former approach in a multi-stage algorithm that also adds heuristics and a stochastic optimization method operating on objective cost functions based on psychoacoustics. The optimization method shows to be able to refine the first estimate given by the deep learning approach and substantially improve the objective metrics, with the additional benefit of reducing the sound design process time. Subjective listening tests are also conducted to gather additional insights on the results.

Index Terms—physics-based acoustic modeling, neural networks, computational sound design, iterative optimization

I. INTRODUCTION

In the recent years a number of advances have been done in several fields of computational acoustics, from the emulation of 3D spaces by finite difference modelling [1] to accurate emulation of nonlinear behaviors of strings [2] and plates [3]. Some of these models rely on an accurate description of a physical setting and their parameters, thus, can be measured from a real settings or purportedly generated to simulate a specific one. Other popular sound synthesis techniques, such as those based on digital waveguide modelling, modal synthesis [4], [5] or a mix of finite difference methods and digital waveguide modelling [6], [7], impose simplifying hypotheses that produce lower-complexity solutions and, hence, a lower computational cost overall. This is done, however, at the cost of a departure from the underlying physics, thus, requiring strategies to estimate coefficients and parameters by matching the outcomes of the model and the target. In other words, the aim is to design a *timbre matching* algorithm, that provides an optimal solution, at least in psychoacoustic terms.

The first known attempt to calibrate a simple physical model using computational intelligence techniques is reported in [8], where a multilayer perceptron (MLP) [9] is trained to estimate parameters of a Karplus-Strong [10] model by learning a perceptual distance obtained from subjective listening tests.

The first three authors are with the Dept. Information Engineering, Università Politecnica delle Marche, the last two are with Viscount International SpA

Recent works [11], [12], extend the topic by introducing additional concepts and techniques, formalizing the goals and problems of the *timbre matching* problem in a computational sound design setting. More specifically, state of the art end-to-end learning [13] has been used with the goal of matching a desired timbre. Convolutional Neural Networks (CNN) have been proposed, which are able to learn acoustic features and provide estimates of the parameters of a flue pipe physical model [14] and the extended Karplus-Strong model. Data visualization techniques such as T-SNE [15] are proposed for dataset exploration as well as objective metrics for evaluating the performance of the estimation algorithm. Other works that are strictly related to computational sound design are reported in [16], [17], [18], [19], where several evolutionary algorithms or linear regression are used to estimate coefficients of different synthesis engines.

In [16] the concept of contrived and non-contrived matching is introduced, which is used also in this work. *Contrived tones* are those belonging to the space of all the signals that can be generated by the synthesis engine, while *non-contrived tones* come from any other sound source (either virtual or real). The paper evaluates results in terms of spectral Euclidean distance. The envelope Euclidean distance is proposed in [18] and the relative spectral error in [17]. In [19] the Source to Distortion Ratio (SDR) [20] is used, however the definition is not clear and there is no detail on how this can be applied to the regression scenario described in the paper.

Further empirical evaluations are conducted in [18] with sound designers, showing that the sound design accuracy of the proposed algorithm is superior to the one obtained by humans. The work reports, however, that the time required for timbre matching by means of the proposed approach is longer than the time required by a sound designer. The reduction of the time to complete the sound design process should be an additional goal for computational sound design processes to be practically relevant.

In the present work we expand in many respects the algorithms detailed in [11], [12], motivated by the need to improve the achieved performance. We continue focusing on the pipe organ tone as a reference use case, but we extend the algorithm for the estimation of the parameters with the introduction of a metaheuristic optimization algorithm that refines the search of a solution. This, in turn, requires introducing metrics in the estimation framework. The evaluation now is performed on a larger number of target sounds. Subjective listening tests are conducted to add further insights to the objective evaluations. Finally, some conclusions are also drawn on the speedup obtained by the computational approach in sound

design, compared to the manual process.

The outline of the paper follows. We first describe the proposed method in all its parts in Section II. Then in Section III we introduce the use case for this paper, the dataset and specific adaptations related to the use case, such as features and metrics. In Section IV we describe the experimental setting and report objective subjective results. The conclusions are drawn in Section V.

II. PROPOSED METHOD

A. Overview

The parameter estimation problem is intended along this paper as the problem of finding a set of parameters θ that allows a physical model $f(\theta)$ to produce an output signal $\hat{s}[n] = f(\theta)$ that matches a target signal $s[n]$ as close as possible. The matching needs to be measured in psychoacoustic terms, as the physical model generally differs from the actual mechanism that produces $s[n]$, thus, a perfect samplewise match cannot be expected. In [12] an approach employing a CNN architecture was devised with the goal of estimating θ from $s[n]$ given prior knowledge of the physical model by a training corpus of parameter sets and signals generated by the physical model.

In this work we propose a multi-stage approach consisting of a Neural Stage (NS), a Selection Stage (SS) and a metaheuristic stage based on a Random Iterative Search (RIS) algorithm, as shown in Figure 1. The NS is composed of fully-connected neural networks that provide different estimations given the input target signal. The SS evaluates each of these estimates and selects, for each note, the best ones, based on one or more acoustic metrics.

The first two stages are meant to perform a *global search*, thus, providing a first solution that can still be improved upon with a local search. For this goal we introduce a general stochastic optimization method, the RIS and an extension thereof named Multi-Objective RIS (MORIS), that looks for a local minimum by iterative stochastic perturbation of the parameters. The motivation behind the introduction of an optimization algorithm is the large acoustical error introduced by small estimation errors for some physical parameters. The optimization stage is expected to refine the results by reducing the estimation errors on a acoustical basis. Both the SS and the MORIS employ acoustic metrics, later described in Section III-E.

B. Neural Stage

Convolutional neural networks were first shown to be capable of estimating a physical model parameters in [11]. One advantage of CNN is the autonomous learning of the input features at the additional expense of large training and testing times. In principle, an autonomous feature learning allows the approach to be employed for different use cases, with the only burden of conducting a partial retraining of the network, applying a transfer learning approach [21], to adapt it to the new data. In other words, it requires no feature selection as the training process guarantees the features that minimize the cost function on a given dataset. Unfortunately this advantage may be vanished by the need for a lengthy hyperparameter

search. In practice, thus, a large number of network models are trained, each with different hyperparameters, among which we can include the choice of the optimizer, of the cost function, the dimensionality of the input (i.e. of the STFT), of the kernels and their strides, of the layers and their number, etc. Furthermore regularization techniques are usually required to avoid overfitting, that prevents a network from generalizing to unseen data. No hyperparameter search method can guarantee the optimal solution, thus only a thorough random search can yield good results, at the expense of computational times.

Differently from other machine learning application fields, in this application field we can rely on some prior knowledge of the data. If this knowledge is applied to the feature extraction phase, efficient digital signal processing can be used to hand-craft features in place of the convolutional layers. This reduces the computational cost but we argue that it also increases the accuracy of the input features. The use of Logmel or STFT spectra of low frequency resolution, that are common to CNN for audio applications, cannot provide accurate information about partials frequency and amplitudes. Furthermore, the max-pooling layers in a CNN although valuable for information compression, reduce the position accuracy of the activation peaks [22], that in the present case may be related to partials, and, thus, may lead to losing vital information for timbre matching and other auditory processing tasks.

For this reason we propose the use of hand-crafted features based on a model of the input signal that may provide more accurate information to the neural network. As an example, if adopting a sinusoidal plus noise model, the tone will be described by a deterministic and a stochastic component [23], yielding features such as the partials frequency, and the evolution of their amplitudes with time, the evolution of the noise energy and the initial ratio between the deterministic and stochastic components. The neural network will, thus, map these data to the model parameters. Since the hand-crafting of the features depends on the input signal model it will be discussed in Section III-D for the application case proposed afterward.

By stripping the convolutional layers from a CNN we retain the fully-connected layers only, what is generally called a multilayer perceptron (MLP). The gained computational resources can be, thus, employed to implement M parallel neural models, each one trained with different data to take advantage of the diversity of multiple alternative estimates. These estimates shall be candidates for the selection stage (SS), discussed in Section II-C.

C. Selection Stage

The selection stage is based on the assumption that M estimates are provided by M neural networks from one input signal. Since the neural networks are all trained differently, some of these estimates, could be better than others. Ideally, the SS is an automation of a manual selection conducted by a human expert that is, however, expensive in terms of time and does not guarantee a unique solution.

In our previous works we remarked that the acoustic error perceived by listeners has no straightforward connection to the

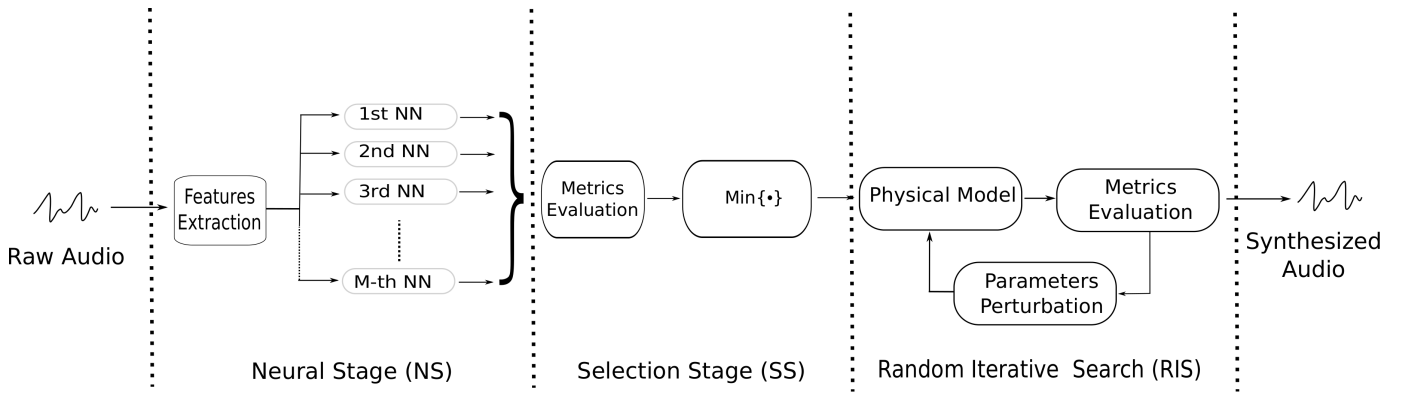


Fig. 1: Multi-Stage Algorithm Overview. Neural Stage (NS) and Selection Stage (SS) are part of a *global search*, the Random Iterative Search (RIS) composes the *local search*.

error on physical model parameters, due to the different role and weight of each parameter in shaping the output signal. For this reason, together with the parameters error, some acoustic metrics were proposed in [11], [12] to evaluate the results. The use of metrics, however, can be successfully employed to automate the selection of the candidates from the previous stage and, thus, improve the algorithm performance without human intervention. The metrics are, thus, employed to select the best candidate among the ones provided in the NS. Prior knowledge of the data is required to devise the metrics. Section III-E will report the ones devised for the use case of Section III.

The selection is based on the iterative comparison described by Algorithm 1 which selects the best matching tone for a given target tone according to the acoustic metrics. Please note that for producing a whole range of tones (e.g. notes on the keyboard range) the proposed algorithm should be repeated for each single tone.

```

Data:  $\{\theta_1, \dots, \theta_M\}$ 
 $\theta_b := \theta_1;$ 
for  $i$  in  $M$  do
  compute  $\hat{s}_i[n] = f(\theta_i);$ 
  evaluate  $d_i = \sum_{k=1}^K a_k J_k(s[n], \hat{s}_i[n]);$ 
  if  $d_i < d_{i-1}$  then
    |  $\theta_b := \theta_i$ 
  end
end
return  $\theta_b;$ 

```

Algorithm 1: Selection Algorithm. The best estimate θ_b is computed using a mix of L metrics weighted by coefficients a_k .

At the output of the selection stage there is a dimensionality reduction of $1/M$ where M is the number of candidates, i.e. of neural networks employed in the NS. The metrics are computed on the signals generated by each one of the candidates. Please note that this requires generating a signal for each candidate by running the physical model, therefore, the computational cost of this stage depends on the cost of the physical model. The weighting of the metrics a_k is arbitrary

and can be imposed by a sound designer supervising the computational sound design process.

D. Random Iterative Search

The outcome of the NS and the SS is an estimate of the physical model parameters that may not be optimal in acoustic terms. The RIS optimization algorithm is intended as a refinement of the estimate that operates iteratively based on the minimization of one acoustic metric (RIS) or multiple acoustic metrics (MORIS), providing a local search that starts from the estimate at the output of the SS. A similar approach to the problem can be found in [16], [17], [18], where evolutionary algorithms are exploited for parameter search. In this case, however, the starting point is not selected randomly but is the outcome of a global search operation that is expected to speed up the convergence of the iterative search.

The basic RIS algorithm and its extension, MORIS, are based on the random perturbation of the parameter space, weighted by the distance calculated from the metrics. The perturbed solution is discarded if its distance from the target signal is increased with respect to the previous step. The entity of the random perturbation, thus, decreases as the algorithm approaches a match. The random perturbation of the parameters at step i is done according to the following equation:

$$\theta_i = \mu d_i \cdot (\theta_b \circ [\mathbf{r} \circ \mathbf{g}]) \quad (1)$$

where:

- θ_b is the best parameter vector achieved so far,
- $\mu < 1$ is an arbitrary step size fixed by the user to improve convergence,
- d_i is the distance at step i ,
- \mathbf{r} is a sparse vector of random values $\in [0, 1]$ of the same size as θ_b ,
- \mathbf{g} is the perturbation vector, with values following a Gaussian distribution and having same size as θ_b .
- \circ is the element-wise Hadamard product operator

The use of a sparse vector \mathbf{r} allows only a random subset of the parameters to be perturbed at each iteration, reducing the dimensionality of the problem.

The difference between RIS and MORIS is in the evaluation of the cost function. While the RIS has a cost function corresponding to a single metric, with the MORIS algorithm, the cost function is composed by a weighted sum of K metrics, i.e.

$$d_i = \sum_{k=1}^K b_k J_k(s[n], \hat{s}_i[n]) \quad (2)$$

where the weights b_k may be different from the weights a_k seen in the SS. The weighting is arbitrary and may be determined to favor the matching of some characteristics of the signal with respect to others.

The general algorithm including both RIS and MORIS variants is reported as Algorithm 2.

```

compute  $\hat{s}_0[n] = f(\theta_0)$ ;
evaluate  $d_0 = \sum_k b_k J_k(s[n], \hat{s}_0[n])$ ;
while  $d_i < \epsilon$  OR maximum iteration reached OR  $p$ 
  iterations reached do
     $\theta_i$  := random perturbation of  $\theta_b$  weighted by  $d_b$ ;
    compute  $\hat{s}_i[n] = f(\theta_i)$ ;
    evaluate  $d_i = \sum_k b_k J_k(s[n], \hat{s}_i[n])$ ;
    if  $d_i < d_{i-1}$  then
       $\theta_b := \theta_i$ ;
       $d_b := d_i$ 
    end
  end

```

Algorithm 2: Multi-Objective Random Iterative Search. The algorithm is based on a random perturbation weighed by the distance of the last best step d_b . It must be noted that the random perturbation is sparse, i.e. not all parameters are perturbed at a given iteration, as reported in Equation (1). Please note that with $K = 1$ the algorithm reduces to RIS.

Both RIS and MORIS work with normalized parameters. Before feeding the physical model with the perturbed parameters; denormalization takes place. Normalization consists in a parameters values adaptation in range $[-1, 1]$ done exploiting parameter-wise value range, denormalization is the inverse process. The stop conditions for the RIS and MORIS algorithms are controlled by the following criteria:

- *Maximum iterations*: the maximum number of iterations to be performed;
- *Distance threshold* ϵ : the maximum distance tolerated, acts as a stop condition if the distance gets lower;
- *Patience iterations* p : consecutive iterations without improvement to wait before early stopping.

Please note that multiple RIS optimization runs can be performed by applying different cost functions each time, seeking minimization of a specific acoustical aspect for each run. Similarly, a single MORIS run can be performed using a cost function composed of a weighted sum of metrics.

III. APPLICATION TO A PIPE ORGAN PHYSICAL MODEL

A. Flue Pipes

A pipe organ generally consists of one or more *manuals* (or *divisions*) and set of *stops*, i.e. groups of pipes. Pipes from a

stop share similar construction characteristics such as materials and shape, and thus, provide similar timbre and sonic qualities. One stop may be assigned to one or more manuals from the organ consolle and can be switched on and off during a performance, allowing changes in dynamics and timbre during the execution of a piece, obtained by summing the stops. This partially addresses the lack of expressivity of the valve opening mechanism that allows no user interaction and is basically dyadic (valve open/closed). The sound design process for the pipe organ can be reduced to the timbre matching of single stops, thus, we shall concentrate on these.

Most stops have one pipe for each note so the experiments reported in IV were made on this kind of stops. Pipes in a stop are tuned as multiple of a base pitch, which is labelled in terms of the length of the longest pipe in the stop, corresponding to a low C. This length is expressed in feet and is approximately 8 feet (8') for a unison stop. Stops may range from 32', i.e. 2 octaves lower than the unison stops, or 1/2', i.e. 4 octaves higher than the *unison* stops. Stops are divided in families depending on their construction features. Flue pipe stops are divided in three families: open stops, closed stops and harmonic stops [24]. The term open and closed refers to the termination of the pipe, which can be open or closed, determining the termination impedance of the air column and, thus, the relation between pitch and pipe length and the harmonic content, with closed stops having no even harmonics. Harmonic stops pipes can be either open or closed. They feature a hole along the bore that determines the pitch.

Each family can be divided in subfamilies depending on tonal or construction characteristics. In this work we take the most common subfamily for each one of the families, namely *Principale* for the open stops, *Bordone* for the closed stops and *Flauto Armonico* from the harmonic stops ¹.

The *Principale* stops are richer in frequency components than *Bordone* stops because the latter are closed pipe stops, typically made in wood. *Bordone* tones are almost exclusively composed of odd harmonic components and have typically darker and softer timbre. *Flauto Armonico* stops can sometimes be composed of closed pipes for the lower part of the keyboard. The presence of a hole and the doubled length yields a sub-harmonic at half the fundamental frequency. These stops often have intermediate qualities and sit in between the open and closed stops.

B. Flue Pipe Modelling

The physical model considered here [14] is meant to simulate a generic flue pipe by means of digital waveguide (DWG) principles. It has been implemented as a standalone C application, allowing it to be run iteratively for use with the proposed algorithm and optimizations have been performed to make the iterations in the MORIS as short as possible.

The model stems from a previous model composed of the feedback coupling between a nonlinear wind jet excitation

¹Please note that these are the names in the Italian organ building tradition. Stop names reported in this work can slightly vary depending on the country of origin (e.g. the French *Flute Harmonique* for *Flauto Armonico* or *Bourdon* for *Bordone*).

mechanism and the passive resonating bore. However, for practical reasons reported in [14], the current model is feedforward, so the wind jet mechanism has been replaced by a signal generator providing its signal-wise emulation. The generator consists of an oscillator with even and odd frequency content control by means of two clipped sine oscillators at f_0 and $2f_0$, a pipe lip shape and size model and a nonlinear filter related to the wind jet angle with respect to the pipe lip.

In flue pipes, noise is generated by air leakage and air hitting the pipe lips. In the model this is simulated by a dedicated computational block interacting with the tonal generation and subject to the resonating cavity. The output is obtained by a pink noise filtered by a feedback delay network which comprises a nonlinear clipping function with thresholds proportional to a rate signal, obtained from high pass filtering and rectifying the fundamental frequency sine tone. This gives so-called *noise granulation*, i.e. the periodically pulsed noise typical of flue pipes.

The passive resonator models the pipe bore by means of DWG modeling, including the effect of dispersion. Of the 58 pipe parameters, 32 are envelope parameters regulating transients times amplitudes, while the remaining part controls static characteristics of the tone. All parameters are time-invariant, thus the evolution of the pipe tone cannot be controlled after the note onset event.

There are dependencies between components of the algorithm which concurrently shape some of the perceptual features of the sound. As an example, variations of the upper lip of the reed and of the bore diameter, e.g., have both impact on the harmonic envelope by creating dips and peaks. The first is modeled in the tonal generator as a delay in the wind path (pipe lip filter), while the second is modeled as the dispersion filter cutoff frequency in the passive resonator.

C. Datasets

1) *Contrived Dataset*: A dataset of physical modelling stops has been created by sound designers in the previous years following traditional sound design procedures and with the goal of obtaining pleasant sounding stops with resemblance to pipes of a certain historical period. This dataset covers most organ families. We refer to this dataset as the *contrived* dataset, being composed of tones that can be perfectly matched by the physical model.

Each item in the dataset is composed of a parameter set and a 4 s-long tone created by the model. Items are labelled according to family, footage and note number (from 0 to 73, corresponding to the range F1-F#7). The availability of a large dataset allows to split it in subsets that have been used for training the neural networks used in the NS.

The subsets used for training follow:

- **Principale**

- subset1: Principale 90 stops (Footage MIX)
- subset2: Principale 132 stops (**8'**)
- subset3: Principale 256 stops (**4'-8'-16'**)
- subset4: Principale 330 stops (All)

- **Bordone**

- subset5: Bordone 56 stops (**8'**)
- subset6: Bordone 150 stops (All)

- **Flauto Armonico**

- subset7: Flauto 21 stops(All)

Additional sets have also been created from summing the above subsets.

2) *Non-Contrived Dataset*: A second dataset has been created from non-contrived sounds. This dataset is composed only of recorded tones. Labels associated to each tone are the note number, the family and footage, using the same convention of the contrived dataset. A selection of material has been conducted from dry samples obtained by near-field recording, excluding most of the ambience and reverb. The portion of the dataset used in this work comes from commercial samples taken from the Caen sampleset from Sonus Paradisi², covering all the stops of an organ by Aristide Cavallè-Coll, one of the most noted organ French Romantic builders. Samples are available from almost all the keys without the use of resampling, thus, providing as a good reference of the original pipe sound. These are used for evaluation in the next sections.

D. Features

The feature set employed for the present use case has been devised considering a flue pipe tone as composed of a short attack transient and a steady state phase. The steady state of pipes is known to be perfectly harmonic. Following this knowledge, a feature set has been crafted that contains spectral information, attack envelope information and coefficients related to the noise. Table I reports further details. The amplitude of the harmonics are meant to describe the steady state periodic spectrum, while the SNR describes the ratio between the latter and the stochastic component of the steady state spectrum. The attack and sustain coefficients track the tone envelope, a useful information for the Neural Network to estimate the envelope parameters of the physical model. Additionally, Logmel coefficients have been added to verify whether they improve the performance or whether they achieve similar performance if employed alone. Figure 2 shows a feature plot where the leftmost part is composed by the logmel coefficients.

TABLE I: Features used in MLP neural network training

Feature Name	Feature Length [<i>min</i> , <i>max</i>]	Description
Harmonics	[10, 100]	Harmonics amplitudes from steady state FFT
SNR	[1]	Stochastic to periodic power ratio
Logmel	[64, 256]	Logmel Spectrum
Attack&Sustain	[12, 24]	Attack and sustain characterization of first P harmonics

²<http://www.sonusparadisi.cz/en/organs/france/caen-st-etienne.html>

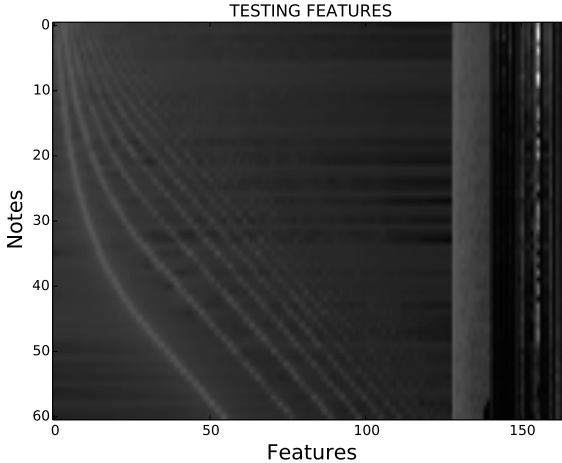


Fig. 2: 2D plot showing features from an entire stop (61 notes). The features are reported along the horizontal axis. The features shown are from left to right: 128 log-Mel coefficients, first 12 harmonics amplitude, SNR, 20 envelope features.

E. Objective Metrics

The use of acoustic metrics is at the core of the SS and the MORIS stages. These are specific for the timbre matching task and may be orthogonal, as is the case with metrics that describe temporal or frequency envelopes, or may concur in describing and giving different weight to similar aspects. The weighting given to each metric concurring to the cost function is arbitrary and must be guided by the sound designer. In the current use case the sound is static and the physical model employed separates the spectral outcome and the temporal evolution, thus allowing to adopt orthogonal metrics.

In the following all the metrics used are listed.

1) *Harmonic Mean Squared Distance Function*: Mean squared distance calculated between harmonics of two periodic signals of same pitch. It measures the difference of each pair of isofrequential harmonics, up to the L -th ones, measured from the DFT magnitude spectrum $S_1(\omega)$ and $S_2(\omega)$ computed on the steady state portion of signals $s_1[n]$ and $s_2[n]$.

$$H_L = \frac{1}{L} \sum_{l=1}^L (S_1(l\omega_0) - S_2(l\omega_0))^2 \quad (3)$$

Along the paper the distance will be denoted as H_H when it is evaluated up to the highest harmonic below the Nyquist frequency.

A weighted harmonic mean squared distance has been also used. This version weights each difference by the amplitude of the harmonic in the target timbre, thus, reducing the importance of the distance when the harmonic to match is low or nearly imperceptible.

$$H_L^W = \frac{1}{L} \sum_{l=1}^L (S_1(l\omega_0) - S_2(l\omega_0))^2 S_1(l\omega_0) \quad (4)$$

2) *Envelope Distance Function*: The envelope distance function measures the difference between two envelopes. In

the present case it is evaluated only for the attack transient. It is evaluated as the squared difference between two envelopes calculated using the Hilbert transform, i.e.:

$$E_D = \sum_{n=0}^{T_s} (|\mathcal{H}(s_1[n])| - |\mathcal{H}(s_2[n])|)^2 \quad (5)$$

Where T_s is the end of attack transient.

Additionally, the same metric can be applied separately to a single harmonic, extracted e.g. by means of heterodyning. In our case the metrics E_1 and E_2 are extracted for the first and second harmonics because these can be independently controlled by the physical model discussed in Section III-B.

IV. EXPERIMENTS AND RESULTS

This section provides implementation details related to the experimental setting. Results are reported exploring both objective and subjective evaluations. For objective evaluations results will be presented employing harmonic mean square distances and the envelope distances, comparing the results with previous works. Subjective tests have been conducted following an approach similar to MUSHRA [25] on 14 subjects with different musical backgrounds.

A. Implementation details

The framework has been implemented in the Python language employing Keras³ libraries and Theano⁴ as a backend, running on a Intel i7 Linux machine equipped with 2 x GTX 970 graphic processing units for neural networks training. The MORIS runs on the same machine but on CPUs. The physical model is implemented as a C++ Linux binary running from console.

A brief overview on training, testing and optimization times is provided. Convolutional Neural Networks (CNN) training and testing times are reported for comparison.

- *CNN Training*: **30-300 [s]** per epoch (depending on the dataset and the network size and parameters).
- *CNN Testing*: **10-30 [s]** (depending on the network size).
- *MLP Training*: **<20 [s]** per epoch (depending on dataset and network).
- *MLP Testing*: **<10 [s]** (depending on network).
- *Selection Algorithm (SA)*: **<5 [s]** per comparison. Selection Algorithm runs on CPU.
- *MORIS*: **3-12 [s]** per Iteration. For every note in iteration a 4 seconds long waveform is synthesized to obtain a set of notes composed of both stationary and transitory state. Times can be reduced generating shorter notes.

All model parameters in the training set are normalized to the range [-1, 1], parameter-wise. The cost function for the training is the mean squared error (MSE), minimized using alternatively one of Stochastic Gradient Descent (SGD) [9], Adam or Adamax [26] optimization algorithms. Parameters

³<http://keras.io>

⁴<http://deeplearning.net/software/theano/>

exploration ranges are reported in table II. Batch normalization [27] and dropout [28] were explored.

TABLE II: Hyperparameters ranges used for the MLP experiments of this work.

Network layout	Layers sizes	Activations
Fully Connected layers: 2, 3, 4,...,12	$2^i, 5 \leq i \leq 12$	<i>tanh</i> or <i>ReLU</i>
Training epochs	Batch size	Optimizer parameters (SGD, Adam, Adamax)
4000, 400 patience Validation split = 10%	10 to 2000	learning rate = $10^i, -8 \leq i \leq -2$ MomentumMax = 0.8, 0.9

A set of 210 Neural Networks were trained with different combinations of hyper-parameters in supervised random configuration. Selected Neural Networks were chosen based on the Mean Absolute Error (MAE) achieved on a target testing set. Every Neural Network is trained on a subset of contrived sounds as reported in Section III-C.

For the Heuristic Search Refinement Algorithm the optimization lasts for 4000 iterations.

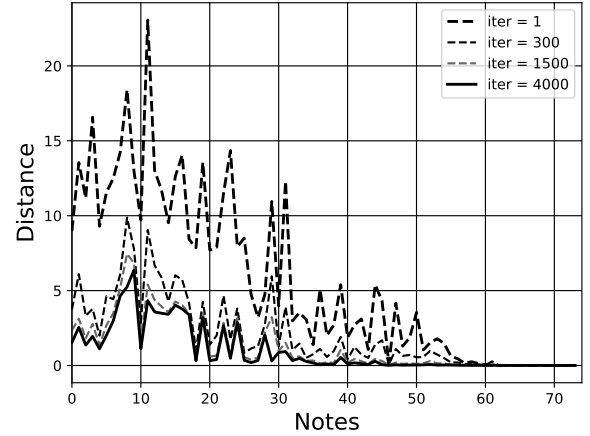
B. Objective Results

This section presents results of the proposed method in acoustic terms employing different metrics. Evaluations are computed and reported separately for each step, from the NS alone to the cascade of NS and SS and finally of all three stages.

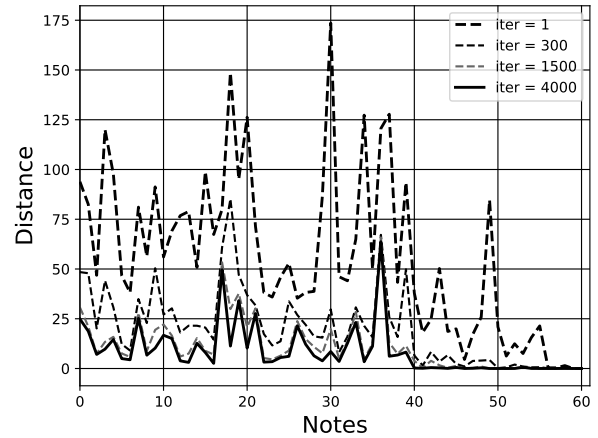
Target stops are both from the contrived and the non-contrived datasets and do not overlap with those used during training of the Neural Networks. Results are given on **8'** stops with fundamental frequency spanning from 43.7 Hz to 2960 Hz. Results are reported for two contrived Principale stops, (*Principale_VS*, *Principale_Stentor_IT*), two non-contrived Principale stops, (*Principal_C_CAEN*, *Salicional_C_CAEN*), one contrived Bordone stop (*Bourdon_G_OS_FR*) and one non-contrived Bordone stop (*CorDeNuit_C_CAEN*), one contrived Flauto Armonico stop (*FluteHarmonique_VS*) and one non-contrived Flauto Armonico stop (*FluteHarmonique_G_CAEN*).

Figure 3 shows the reduction of the acoustic distance during MORIS optimization for a contrived and a non-contrived stop. With a reduction of the distance between target and matched tones, the improvement gets reduced. This is due to the error-weighting done by the MORIS algorithm. As shown, the reduction of the distance can be of an one order of magnitude.

Table III reports results in terms of H_H , H_{10} and H_{10}^W , while Table IV reports the results in terms of the envelope metrics. Tests T1, T2 and T3 are reported, with T1 reporting the results of the best single Neural Network, T2 reporting the outcome of the SS, thus, exploiting all Neural Networks. T3 is the outcome of the MORIS. Please note that two runs are performed, a first MORIS run minimizing harmonics distances and a second MORIS minimizing the envelope distances on the first and second harmonics and on the whole waveform. As expected, convergence with MORIS is reached in shorter time if the previous stages are able to provide a good estimation of the target tones.



(a) Objective acoustic Error calculated from H , H_{10} and H_{10}^W metrics on *contrived* stop using weights respectively of [1, 1, 3].



(b) Objective acoustic Error calculated from H , H_{10} and H_{10}^W metrics on *non-contrived* stop using weights respectively of [1, 1, 3].

Fig. 3: The reduction of the acoustic distance in the MORIS process for a contrived (a) and non-contrived (b) stop. The distance shown is measured at the beginning of the process and after 300, 1500 and 4000 iterations. The cost function to minimize is the sum of H , H_{10} and H_{10}^W , shown for each one of the notes of a stop (horizontal axis). For the contrived stop the note range is F1-F#7, while for the non-contrived stop the note range is C2-C7.

In most of the presented results there is a remarkable improvement from T1 to T2 output. In those cases where the improvement is little, e.g. with contrived Principale stops, the estimation provided by a single Neural Network was able to provide results above the average. T3 gives best results for all tests, in many cases providing a large distance reduction from T2. For what concerns the envelope distance an important improvement is obtained using a MORIS with envelope metrics as a cost function. From informal listening tests the last stage seems to allow, for contrived stops, to reach a nearly perfect psychoacoustic matching of the timbre, with H_H , H_{10} and H_{10}^W metrics reaching 1 dB or below.

For Bordone stops, the larger errors can be motivated by their distinctive properties, i.e. the lack of even harmonics and the low number of harmonics, thus making the distance estimate altered by large random differences in the spectral regions between odd harmonics or above the last harmonic. Even though a custom metric (e.g. based only on odd harmonics up to the last one present) would produce better results, we decided to keep the same metric for coherence with the other stops.

As a final remark, contrived tones score better than non-contrived ones, as expected. Timbre matching for contrived tones is nearly optimal, suggesting that the reduced scores obtained with non-contrived stops are due to the physical model limitations. In the authors' opinion this highlights another valuable contribution of the proposed method: not only it can be used for the timbre matching, but also to spot and analyze deficiencies of the physical model under exam, by analysis of the differences between the best match obtained with the proposed approach and the target tone.

C. Subjective Tests

Listening tests have been conducted to assess the effect of the reduced acoustic distances in psychoacoustic terms. The subjective tests are inspired by the MUSHRA method [25]. With MUSHRA a user is exposed to several stimuli, and he/she must rate the similarity of each of them with respect to a reference tone using a 1-100 scale. The method also requires that at least one *anchor* and a hidden copy of the reference are provided among the stimuli. The mandatory anchor is a tone providing a bottom line to the test, and this is done by degrading its quality using a 3.5 kHz low-pass filtered version of the reference. This fits well the use case of audio coding algorithms or sound reproduction systems, where one of the quality criteria is the bandwidth of the audio output, however in our case this choice is not perfectly viable because many organ tones may have very low energy over 3.5 kHz resulting in a hardly perceptible degradation. The recommendations [25] suggest the addition of other types of anchors providing similar types of impairments as the system under test, e.g. additional noise, packet loss and dropouts in the case of audio transmission systems. Following these guidelines and considering that the kind of impairment provided by a bad timbre matching can be, e.g. the presence of excess wind noise and a mismatch of the harmonic content, we devised an anchor by manually modifying a *Principale* tone. The noise gain in the physical model was raised in order to have an RMS value that is +30dB with respect to the harmonic component and the wind nonlinearity was modified so that only the first and second harmonics were generated.

The stimuli under test consisted in a tone generated by the CNN estimate as in the End-to-End algorithm in [12] and a tone generated by the output of the proposed algorithm (indicated as PROP) including all stages. To resume, the subjects were exposed for each screen of the test to the reference tone and the following stimuli in random order: a hidden reference tone, the proposed anchor, the CNN estimation and the full NS+SS+MORIS estimation. The test consisted of eight screens

with a first warm-up screen, not employed in the evaluation. Four screens were related to a contrived reference tone and four to a non-contrived reference tone. The whole test took 15 minutes per subject on average. Tests have been conducted on 20 subjects, 15 male and 5 female aged 16-53 with varying musical background. After the tests have been completed 6 of the subjects were discarded, following MUSHRA guidelines, because they were not able to reliably repeat the assessment of the hidden reference, specifically, they rated it for more than 15% of the test items with a score lower than 90.

Table V reports data for each of the 14 selected subjects, providing the average rating for CNN tones and PROP tones for each subject, the musical background of each subject and the average and standard deviation of the CNN and PROP tones for the whole session of tests. Every single subject evaluated the CNN results worse than PROP results. The average distance is 16.2 and the difference between the two approaches is statistically significant. The significance test have been done considering the null hypothesis $h_0 : \mu = \overline{PROP} - \overline{CNN} < 0$ with a p-value of 0.1, where \overline{CNN} and \overline{PROP} are respectively average values of CNN and PROP per subject.

Statistical test on hypothesis h_0 has been conducted exploiting a Student's t-distribution with 14 degrees of freedom.

D. Impact on the Sound Design Process

Before the introduction of computational sound design techniques, the sound design process was completely manual, based on the knowledge and the skills of the sound designer and never had the goal of matching a set of samples. Therefore, the development of the computational sound design approach described above has an impact on the process of creating sound libraries that can be played by musicians. We report some qualitative information from informal discussion with the sound design team that developed the model and the sound libraries commercially available for the aforementioned physical model since year 2004.

Before the introduction of timbre matching techniques a sound designer followed these steps:

- select a reference stop family of a specific style, related to either historical or geographical factors influencing the target timbre;
- start from a template of parameters or a similar stop if already designed;
- manually interact with a graphical software to alter the parameters of a note based on the knowledge of the physical model and the causal relation between parameters and sound until a desired timbre is obtained;
- repeat previous step for a subset of notes;
- interpolate between the selected notes to obtain values for the rest of the notes in the keyboard range, eventually adding some random fluctuations.

Please note that the reference stop may not be an existing stop, or a stop available to the sound designer in form of recorded tones, but it may be a mental representation of a prototype sound from a specific style or historical organ builder.

Contrived				Non-Contrived			
	H_H	H_{10}	H_{10}^W		H_H	H_{10}	H_{10}^W
<i>Principale VS 8' [P]</i>				<i>Principal 8' (Caen) [P]</i>			
[12]	11.04 dB	12.78 dB	16.95 dB	[12]	32.56 dB	29.51 dB	68.53 dB
NS	4.91 dB	2.44 dB	3.36 dB	NS	25.69 dB	23.58 dB	40.94 dB
SS	2.95 dB	1.06 dB	1.41 dB	SS	14.24 dB	10.14 dB	21.89 dB
MORIS	2.32 dB	1.01 dB	1.00 dB	MORIS	4.58 dB	2.60 dB	3.41 dB
<i>Principale Stentor 8' [P]</i>				<i>Salicional 8' (Caen) [P]</i>			
[12]	25.13 dB	28.47 dB	52.07 dB	[12]	182.66 dB	232.84 dB	1163.57 dB
NS	3.86 dB	1.58 dB	3.31 dB	NS	17.67 dB	13.26 dB	30.20 dB
SS	3.26 dB	1.53 dB	2.36 dB	SS	11.25 dB	8.08 dB	15.56 dB
MORIS	1.32 dB	0.52 dB	0.77 dB	MORIS	4.93 dB	3.48 dB	3.87 dB
<i>Bourdon GO FR 8' [B]</i>				<i>Cor de Nuit 8' (Caen) [B]</i>			
NS	46.66 dB	53.31 dB	115.49 dB	NS	44.71 dB	50.16 dB	88.65 dB
SS	21.65 dB	21.11 dB	24.73 dB	SS	24.74 dB	21.21 dB	32.96 dB
MORIS	11.50	8.63 dB	10.18 dB	MORIS	8.84 dB	4.60 dB	4.87 dB
<i>Flute Harmonique VS 8' [FA]</i>				<i>Flute Harmonique 8' (Caen) [FA]</i>			
NS	10.90 dB	5.34 dB	16.67 dB	NS	36.68 dB	56.87 dB	59.32 dB
SS	8.58 dB	2.30 dB	6.93 dB	SS	19.91 dB	13.89 dB	29.78 dB
MORIS	1.40 dB	0.49 dB	0.38 dB	MORIS	15.86 dB	11.85 dB	12.27 dB

TABLE III: Timbre matching results reported in terms of harmonic distance at the output of each stage of the proposed approach for stops belonging to the Principale (P), Bordone (B) and Flauto Armonico (FA) subfamilies. Where available, the results from the end-to-end approach of [12] are reported. Please note that NS is the outcome of the best single neural network among all the neural networks used for the subsequent SS. MORIS has been carried on for 4000 iterations.

Contrived				Non-Contrived			
	E_2	E_1	E_D		E_2	E_1	E_D
<i>Principale Stentor 8' [P]</i>				<i>Salicional 8' (Caen) [P]</i>			
SS	230.47	86.71	394.18	SS	2053.02	6430.48	3211.78
MORIS	5.48	9.59	341.12	MORIS	1380.81	1633.63	2326.01

TABLE IV: Timbre matching results reported in terms of envelope distance at the output of the SS and MORIS stages, for two Principale stops. Results are presented exploiting envelope distances. The MORIS stage has been run for 300 iterations with the E_D , E_1 and E_2 as cost function. Results are presented for two stops only for conciseness, but similar results are found with all other tested stops.

Subject	CNN	PROP	Exp(Y)
S1	40.625	66.500	12
S2	50.125	71.750	9
S3	68.125	80.000	12
S4	58.125	75.375	0
S5	53.125	58.625	19
S6	58.500	60.250	9
S7	51.000	64.375	30
S8	30.125	55.875	0
S9	53.000	63.375	14
S10	32.500	63.125	0
S11	48.625	74.125	10
S12	44.769	56.538	38
S13	45.538	66.769	40
S14	53.538	66.308	38
Overall Average	49.7	65.9	
Standard Deviation	10.4	7.2	
Average Difference	16.2		

TABLE V: Subjective test summary table. Per-subject and averaged test values are reported. The last column reports the musical experience for each subject expressed as the number of years of study and practice.

Development times for such an approach are strongly dependent on human factors such as fatigue, experience, knowledge of the physical model and efficiency of the graphical software interface. From the informal discussion it seems that preparing a complete stop required an effort that is of the order of magnitude of a working day (8 hours) split in several sessions

to recover from fatigue, while with the proposed approach and the current computational resources one stop can be prepared in approximately 5 minutes to which some human effort must be added to judge on the result and conduct some final adjustments.

To conclude, it must be noted that the computational process allows for an objective result, while, previously, target tones were seldom used, as the matching would hardly be feasible in a reasonable amount of time. As a downside, the objective approach requires data, specifically, good quality recordings of single tones, not always available at ease. It is worth noting that the expertise of the sound designer is still very valuable even with the proposed timbre matching approach as he/she is still responsible for all the design choices and the supervision of the computational work.

V. CONCLUSIONS

In this paper a novel multi-stage estimation algorithm is presented and applied to the physical model parameters estimation task. The first stage consists in a refinement of previous deep learning techniques, where feature learning is replaced by hand-crafted features. Hyperparameter diversity is employed in the subsequent selection stage by picking the best note estimate from a number of differently trained and crafted neural networks. Finally results are refined using an optimization algorithm that employs acoustic distances as cost functions. The first two stages perform a global search in the

physical model parameter space, while the last stage performs a local search that converges to a suboptimal solution.

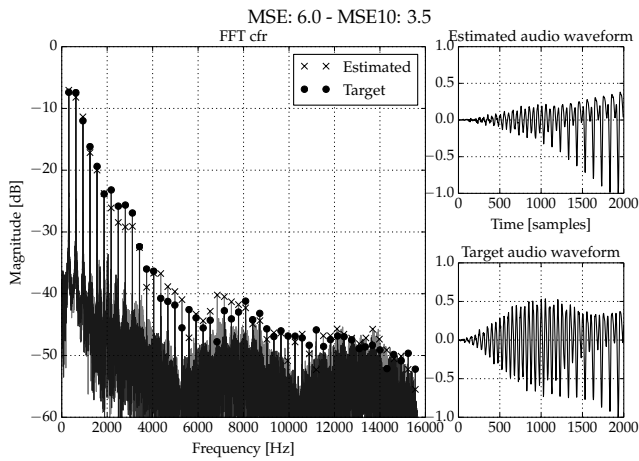
The algorithm has been validated on a flue pipe physical model as in previous works. The approach is tested on contrived and non-contrived sounds, showing that a large improvement with respect to recent techniques is achieved in both cases. Listening tests have been performed to assess the improvement given by the proposed algorithm with respect to the previous end-to-end algorithm, showing a clear preference of the subjects for the timbre matching provided by the proposed algorithm.

An argument can be made that, when the matching of contrived tones is nearly optimal, the approach can highlight the limitations of the physical model, thus, providing useful insights for the sound designer to improve the model. More experiments to be conducted on open-sourced physical models are on the way.

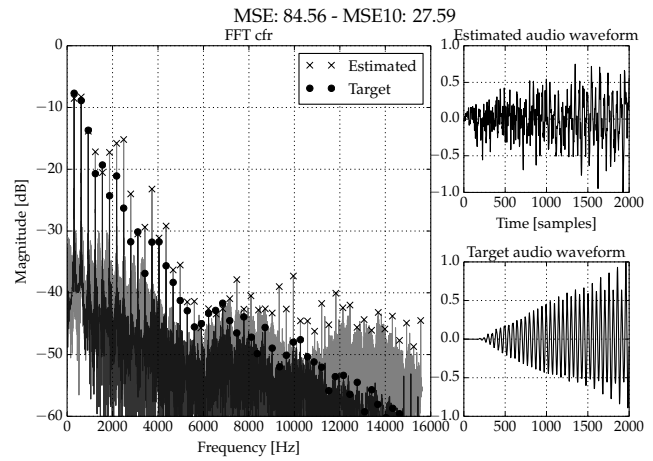
As a last remark, the change from the learned features used in [12] to the hand-crafted features is able itself to largely improve the estimation performance. This result may be surprising, given the current trends towards autonomous feature learning in the computational audio processing field. However, other authors have argued that the 2D convolutional approach, as developed by image processing researchers, is not adequate for audio processing as it does not account for time-frequency anisotropies, and, thus, several modifications of the convolutional approach have been already proposed both on 2D and 1D audio representations [29], [30], [31], [32]. More investigation in the machine listening field is required to understand how an accurate computational auditory model can be built to be exploited in the timbre matching task and supersede hand-crafted features.

REFERENCES

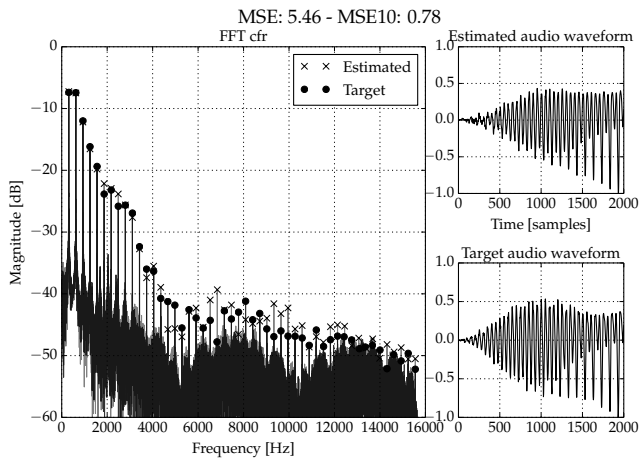
- [1] Brian Hamilton and Stefan Bilbao, "FDTD methods for 3-D room acoustics simulation with high-order accuracy in space and time," *IEEE/ACM Transactions on Audio, Speech, and Language Processing*, vol. 25, no. 11, pp. 2112–2124, Nov 2017.
- [2] Charlotte Desvages and Stefan Bilbao, "Two-polarisation physical model of bowed strings with nonlinear contact and friction forces, and application to gesture-based sound synthesis," *Applied Sciences*, vol. 6, no. 5, 2016.
- [3] A Torin and M Newton, "Nonlinear effects in drum membranes," in *Proceedings of the International Symposium on Musical Acoustics*, 2014, pp. 107–112.
- [4] B. Bank, S. Zambon, and F. Fontana, "A modal-based real-time piano synthesizer," *IEEE Trans. Audio Speech Lang. Processing*, vol. 18, no. 4, pp. 809–821, 2010.
- [5] Stefano Gabrielli, Leonardo Gabrielli, and Balazs Bank, "Expressive physical modeling of keyboard instruments: From theory to implementation," in *Audio Engineering Society Convention 134*. Audio Engineering Society, 2013.
- [6] M. Karjalainen and C. Erkut, "Digital Waveguides versus Finite Difference Structures: Equivalence and Mixed Modeling," *EURASIP Journal on Advances in Signal Processing*, no. 7, pp. 978–989, 2004.
- [7] Leonardo Gabrielli, Luca Remaggi, Stefano Squartini, and Vesa Välimäki, "A finite difference method for the excitation of a digital waveguide string model," in *AES 134th Convention*, may 2013.
- [8] Ali Taylan Cemgil and Cumhur Erkut, "Calibration of physical models using artificial neural networks with application to plucked string instruments," *Proc. Intl. Symposium on Musical Acoustics (ISMA)*, vol. 19, pp. 213–218, 1997.
- [9] David Rumelhart, Geoffrey Hinton, and Ronald Williams, "Learning representations by back-propagating errors," *Nature*, vol. 323, pp. 533–536, Oct. 1986.
- [10] Kevin Karplus and Alex Strong, "Digital synthesis of plucked-string and drum timbres," *Computer Music Journal* 7(2): 43-55, 1983.
- [11] Leonardo Gabrielli, Stefano Tomassetti, Carlo Zinato, and Stefano Squartini, "Introducing deep machine learning for parameter estimation in physical modelling," in *Digital Audio Effects (DAFX)*, 2017.
- [12] L. Gabrielli, S. Tomassetti, C. Zinato, and F. Piazza, "End-to-end learning for physics-based acoustic modeling," *IEEE Transactions on Emerging Topics in Computational Intelligence*, vol. 2, no. 2, pp. 160–170, April 2018.
- [13] Ian Goodfellow, Yoshua Bengio, and Aaron Courville, *Deep Learning*, MIT Press, 2016.
- [14] Carlo Zinato, "Method and electronic device used to synthesise the sound of church organ flue pipes by taking advantage of the physical modeling technique of acoustic instruments," Oct. 28 2008, US Patent 7,442,869.
- [15] Laurens van der Maaten and Geoffrey Hinton, "Visualizing data using t-SNE," *Journal of Machine Learning Research*, vol. 9, no. Nov, pp. 2579–2605, 2008.
- [16] Thomas J Mitchell and David P Creasey, "Evolutionary sound matching: A test methodology and comparative study," in *Machine Learning and Applications, 2007. ICMLA 2007. Sixth International Conference on*. IEEE, 2007, pp. 229–234.
- [17] Thomas Mitchell, "Automated evolutionary synthesis matching," *Soft Computing*, vol. 16, no. 12, pp. 2057–2070, 2012.
- [18] Kıvanç Tatar, Matthieu Macret, and Philippe Pasquier, "Automatic synthesizer preset generation with presetgen," *Journal of New Music Research*, vol. 45, no. 2, pp. 124–144, 2016.
- [19] Katsutoshi Itoyama and Hiroshi G Okuno, "Parameter estimation of virtual musical instrument synthesizers," in *Proc. of the International Computer Music Conference (ICMC)*, 2014.
- [20] E. Vincent, R. Gribonval, and C. Fevotte, "Performance measurement in blind audio source separation," *IEEE Transactions on Audio, Speech, and Language Processing*, vol. 14, no. 4, pp. 1462–1469, July 2006.
- [21] Sebastian Thrun and Lorien Pratt, *Learning to Learn*, Springer Science & Business Media, 2012.
- [22] Sara Sabour, Nicholas Frosst, and Geoffrey E Hinton, "Dynamic routing between capsules," in *Advances in Neural Information Processing Systems*, 2017, pp. 3856–3866.
- [23] Xavier Serra et al., "Musical sound modeling with sinusoids plus noise," in *Musical signal processing*, Curtis Roads, Stephen Travis Pope, Aldo Piccialli, and Giovanni de Poli, Eds., chapter PartI-Ch.3, pp. 91–122. Routledge, 1997.
- [24] George Ashdown Audsley, *The Art of Organ Building: A Comprehensive Historical, Theoretical, and Practical Treatise on the Tonal Appointment and Mechanical Construction of Concert-Room, Church, and Chamber Organs*, Dover Publications, 1905.
- [25] ITU-R, "Method for the subjective assessment of intermediate quality level of audio system," Recommendation BS.1534-3, International Telecommunication Union, Geneva, Oct. 2015.
- [26] Diederik Kingma and Jimmy Ba, "Adam: A method for stochastic optimization," *arXiv preprint arXiv:1412.6980*, 2014.
- [27] S. Ioffe and C. Szegedy, "Batch normalization: Accelerating deep network training by reducing internal covariate shift," *arXiv preprint arXiv:1502.03167*, 2015.
- [28] Nitish Srivastava, Geoffrey Hinton, Alex Krizhevsky, Ilya Sutskever, and Ruslan Salakhutdinov, "Dropout: A simple way to prevent neural networks from overfitting," *The Journal of Machine Learning Research*, vol. 15, no. 1, pp. 1929–1958, 2014.
- [29] Jordi Pons and Xavier Serra, "Designing efficient architectures for modeling temporal features with convolutional neural networks," in *IEEE International Conference on Acoustics, Speech, and Signal Processing*, 2017.
- [30] Jordi Pons, Olga Slizovskaia, Rong Gong, Emilia Gómez, and Xavier Serra, "Timbre analysis of music audio signals with convolutional neural networks," *25th European Signal Processing Conference, EUSIPCO*, 2017.
- [31] Jongpil Lee, Jiyoung Park, Keunhyoung Luke Kim, and Juhan Nam, "Sample-level deep convolutional neural networks for music auto-tagging using raw waveforms," *arXiv preprint arXiv:1703.01789*, 2017.
- [32] Aaron van den Oord, Sander Dieleman, Heiga Zen, Karen Simonyan, Oriol Vinyals, Alex Graves, Nal Kalchbrenner, Andrew Senior, and Koray Kavukcuoglu, "Wavenet: A generative model for raw audio," *white paper, available online at https://arxiv.org/pdf/1609.03499.pdf*, 2016.



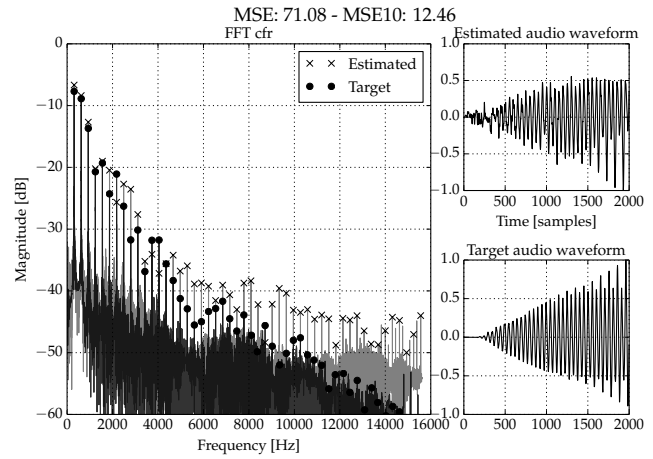
(a)



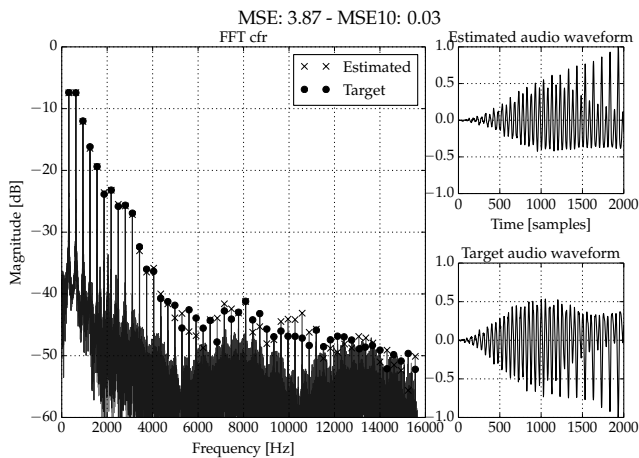
(a)



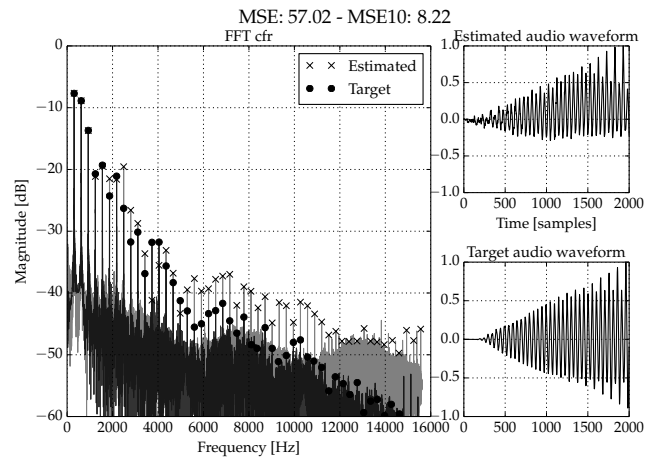
(b)



(b)



(c)



(c)

Fig. 4: Spectra and attack transient in the time domain for contrived *Principale_VS* D#4 tone (a) from T1, (b) from T2 and (c) from T3. H and H_{10} are respectively 6.00 dB, 3.50 dB (a), 5.46 dB, 0.78 dB for (b) and 3.87 dB and 0.03 dB for (c).

Fig. 5: Spectra and attack transient in the time domain for non-contrived *Salicional_C_CAEN* D#4 tone (a) from T1, (b) from T2 and (c) from T3. H and H_{10} are respectively 84.56 dB, 27.59 dB (a), 71.08 dB, 12.46 dB for (b) and 57.02 dB and 8.22 dB for (c).